

Optimal restoration of noisy 3D X-ray data via shearlet decompositions

Demetrio Labate^a, Glenn R. Easley^b, Kanghui Guo^c

^a University of Houston

^b MITRE

^c Missouri State University

ABSTRACT

In a recent work, it was shown that the shearlet representation provides a useful formula for the reconstruction of 3D objects from their X-ray projections. One major advantage of this approach is that it yields a near-optimal rate of convergence in estimating piecewise smooth objects from 3D X-ray projections which are corrupted by white Gaussian noise. In this work, we provide numerical demonstrations to illustrate the effectiveness of this method and its performance as compared with other X-ray data restoration algorithms.

Keywords: shearlets, wavelets, X-ray

1. INTRODUCTION

The Radon and X-ray transforms are the mathematical models underlying computed tomography (CT), a method to determine the structural properties of solid objects from their projected information which is extensively used in medical imaging (diagnostic radiology) and in industrial nondestructive testing (quality control). In the 3-dimensional setting, in particular, let the density function f of the object to be recovered be a compactly supported integrable function. The *X-ray transform* P of f at (Θ, x) is the line integral of f over the straight lines through the point $x \in \mathbb{R}^3$ with direction $\Theta \in S^2$, defined by

$$P(\Theta, x)f = \int_{\mathbb{R}} f(t\Theta + x) dt.$$

This is also called the projection of f onto Θ^\perp , the plane having normal direction Θ . Note that $Pf(\Theta, x)$ does not change if x is moved in the direction Θ . Hence, x is normally restricted to Θ^\perp so that Pf is a function on the *tangent bundle* $\mathcal{T} = \{(\Theta, x) : \Theta \in S^2, x \in \Theta^\perp\}$.

The problem of interest is the reconstruction of f from its projected information and this requires the formal inversion of the X-ray transform. This problem has an analytic solution and, in the 2D setting, an inversion formula was derived by J. Radon¹⁵ already in 1917. However, the inversion of the Radon and X-ray transforms is an ill-posed problem whose computation is very sensitive to small perturbations in the data. Since, in practical applications, the projected information is known on a discrete set only, with a limited accuracy, and is corrupted by noise, the inversion process requires an appropriate regularization to accurately recover the unknown function f without blowing up the noise during reconstruction.

Several methods have been introduced to regularize the inverse problem associated with the Radon and X-ray transforms, including Fourier methods, backprojection and singular value decomposition.¹³ The drawback of these classical methods is that they typically filter out the high frequency features of the projected data, with the result that there is a loss of fine-scale detail in the reconstructed images. In contrast to these methods that use basis functions depending solely on the operator to regularize the inversion, originally proposed by Donoho,³ offers an alternative strategy to inverse problems which takes advantage the estimating capabilities of a representation best suited to approximate the solution. This approach was applied to the study of the 2D Radon transform by Candès and Donoho¹ and by the authors,^{2,4} who have recently extended this approach to

the X-ray transform in the 3D setting.⁶ These new methods exploit the properties of curvelets and shearlets, a new generation of multiscale representation systems, to derive reconstruction formulas which have particularly robust in the case of noisy Radon and X-ray data corrupted.

In this paper, we focus on the CT reconstruction problem in the 3D setting, which is the case of most interest in practical applications. In a recent work,⁶ the authors have employed the multidimensional shearlet representation within the framework of the wavelet-vaguelettes decomposition to derive a new expansion formula for the 3D X-ray transform. Taking advantage of the special ability of 3D shearlets to sparsely represent piecewise smooth data, they derived an algorithm for the inversion of X-ray transform from noisy X-ray projections whose error rate is provably near-optimal. This algorithm is based on a thresholding scheme on the noisy shearlet coefficients associated with the decomposition of the 3D X-ray transform. Specifically, for a given noise level ε , the proposed thresholding scheme can be tuned so that the estimator will attain the essentially optimal mean square error (MSE) $O(\log(\varepsilon^{-1})\varepsilon^{2/3})$, as $\varepsilon \rightarrow 0$. This is the first published result to yield an essentially optimal MSE rate for the recovery of noisy 3D x-ray data.

The goal of this paper is to present the first numerical implementation attempting to take advantage of this new approach. Note that the theoretical result was derived under ‘academic’ assumption that the X-ray projections are known for all values (Θ, x) . In the following, we consider the more realistic setting of spiral tomography, where the X-ray radiation sources are assumed to be located along a spiral containing the object of interest. We show that also in this setting a shearlet-based approach provides a very effective method for 3D reconstruction from X-ray projected data which are corrupted by additive white Gaussian noise.

The paper is organized as follows. In section 2, we recall the construction of 3D shearlets. In section 3, we recall the main theoretical results about the shearlet-based representation of the X-ray transform and its application to the optimal reconstruction from noisy X-ray data. Finally, in section 4, we present our new numerical demonstrations.

2. THE SHEARLET REPRESENTATION

In dimension $D = 3$, a shearlet system is obtained by appropriately combining 3 systems of functions associated with the following pyramidal regions in the 3D Fourier space:

$$\begin{aligned}\mathcal{P}_1 &= \left\{ (\xi_1, \xi_2, \xi_3) \in \mathbb{R}^3 : \left| \frac{\xi_2}{\xi_1} \right| \leq 1, \left| \frac{\xi_3}{\xi_1} \right| \leq 1 \right\}, \\ \mathcal{P}_2 &= \left\{ (\xi_1, \xi_2, \xi_3) \in \mathbb{R}^3 : \left| \frac{\xi_1}{\xi_2} \right| < 1, \left| \frac{\xi_3}{\xi_2} \right| \leq 1 \right\}, \\ \mathcal{P}_3 &= \left\{ (\xi_1, \xi_2, \xi_3) \in \mathbb{R}^3 : \left| \frac{\xi_1}{\xi_3} \right| < 1, \left| \frac{\xi_2}{\xi_3} \right| < 1 \right\}.\end{aligned}$$

To define such systems, let b be a univariate function such that $\hat{b} \in C^\infty$, $0 \leq \hat{b} \leq 1$, $\hat{b} = 1$ on $[-\frac{1}{16}, \frac{1}{16}]$ and $\hat{b} = 0$ outside the interval $[-\frac{1}{8}, \frac{1}{8}]$. For $\xi = (\xi_1, \xi_2, \xi_3) \in \mathbb{R}^3$, define ϕ by

$$\widehat{\phi}(\xi) = \widehat{\phi}(\xi_1, \xi_2, \xi_3) = \hat{b}(\xi_1) \hat{b}(\xi_2) \hat{b}(\xi_3) \quad (1)$$

and $W(\xi) = \sqrt{|\widehat{\phi}(2^{-2}\xi)|^2 - |\widehat{\phi}(\xi)|^2}$. It follows that $|\widehat{\phi}(\xi)|^2 + \sum_{j \geq 0} |W(2^{-2j}\xi)|^2 = 1$ for $\xi \in \mathbb{R}^3$.

Notice that each function $W_j = W(2^{-2j} \cdot)$ has support in the Cartesian corona

$$C_j = [-2^{-2j-1}, 2^{-2j-1}]^3 \setminus [-2^{-2j-4}, 2^{-2j-4}]^3 \subset \mathbb{R}^3, \quad (2)$$

and the functions W_j^2 , $j \geq 0$, produce a smooth tiling of the frequency plane into Cartesian coronae:

$$\sum_{j \geq 0} |W(2^{-2j}\xi)|^2 = 1 \quad \text{for } \xi \in \mathbb{R}^3 \setminus [-\frac{1}{8}, \frac{1}{8}]^3. \quad (3)$$

Next, let $v \in C^\infty(\mathbb{R})$ be such that $v(0) = 1$, $v^{(n)}(0) = 0$ for all $n \geq 1$, $\text{supp } v \subset [-1, 1]$ and

$$|v(u-1)|^2 + |v(u)|^2 + |v(u+1)|^2 = 1 \quad \text{for } |u| \leq 1. \quad (4)$$

Hence, for $d = 1, 2, 3$, $\ell = (\ell_1, \ell_2) \in \mathbb{Z}^2$, the 3D *shearlet systems associated with the pyramidal regions* \mathcal{P}_d are defined as the collections

$$\{\psi_{j,\ell,k}^{(d)} : j \geq 0, -2^j \leq \ell_1, \ell_2 \leq 2^j, k \in \mathbb{Z}^3\}, \quad (5)$$

where

$$\hat{\psi}_{j,\ell,k}^{(d)}(\xi) = |\det A_{(d)}|^{-j/2} W(2^{-2j}\xi) V_{(d)}(\xi A_{(d)}^{-j} B_{(d)}^{[-\ell]}) e^{2\pi i \xi A_{(d)}^{-j} B_{(d)}^{[-\ell]} k}, \quad (6)$$

$V_{(1)}(\xi_1, \xi_2, \xi_3) = v(\frac{\xi_2}{\xi_1})v(\frac{\xi_3}{\xi_1})$, $V_{(2)}(\xi_1, \xi_2, \xi_3) = v(\frac{\xi_1}{\xi_2})v(\frac{\xi_3}{\xi_2})$, $V_{(3)}(\xi_1, \xi_2, \xi_3) = v(\frac{\xi_1}{\xi_3})v(\frac{\xi_2}{\xi_3})$, the anisotropic dilation matrices $A_{(d)}$ are given by

$$A_{(1)} = \begin{pmatrix} 4 & 0 & 0 \\ 0 & 2 & 0 \\ 0 & 0 & 2 \end{pmatrix}, A_{(2)} = \begin{pmatrix} 2 & 0 & 0 \\ 0 & 4 & 0 \\ 0 & 0 & 2 \end{pmatrix}, A_{(3)} = \begin{pmatrix} 2 & 0 & 0 \\ 0 & 2 & 0 \\ 0 & 0 & 4 \end{pmatrix},$$

and the *shearing matrices* are defined by

$$B_{(1)}^{[\ell]} = \begin{pmatrix} 1 & \ell_1 & \ell_2 \\ 0 & 1 & 0 \\ 0 & 0 & 1 \end{pmatrix}, B_{(2)}^{[\ell]} = \begin{pmatrix} 1 & 0 & 0 \\ \ell_1 & 1 & \ell_2 \\ 0 & 0 & 1 \end{pmatrix}, B_{(3)}^{[\ell]} = \begin{pmatrix} 1 & 0 & 0 \\ 0 & 1 & 0 \\ \ell_1 & \ell_2 & 1 \end{pmatrix}.$$

Notice that $(B_{(d)}^{[\ell]})^{-1} = B_{(d)}^{[-\ell]}$.

Due to the support conditions on W and v , the shearlets (5) are band-limited. In particular, for $d = 1$, the functions $\hat{\psi}_{j,\ell,k}^{(1)}(\xi)$ can be written explicitly as

$$\hat{\psi}_{j,\ell_1,\ell_2,k}^{(1)}(\xi) = 2^{-2j} W(2^{-2j}\xi) v\left(2^j \frac{\xi_2}{\xi_1} - \ell_1\right) v\left(2^j \frac{\xi_3}{\xi_1} - \ell_2\right) e^{2\pi i \xi A_{(1)}^{-j} B_{(1)}^{[-\ell_1, -\ell_2]} k}. \quad (7)$$

It follows that their supports are the trapezoidal regions

$$\{(\xi_1, \xi_2, \xi_3) : \xi_1 \in [-2^{2j-1}, -2^{2j-4}] \cup [2^{2j-4}, 2^{2j-1}], |\frac{\xi_2}{\xi_1} - \ell_1 2^{-j}| \leq 2^{-j}, |\frac{\xi_3}{\xi_1} - \ell_2 2^{-j}| \leq 2^{-j}\},$$

which are contained inside the pyramid \mathcal{P}_1 . As $a \rightarrow 0$, these trapezoidal support regions become increasingly more elongated, with the orientations controlled by ℓ_1, ℓ_2 (see Fig. 1).

A Parseval frame of shearlets for $L^2(\mathbb{R}^3)$ is obtained by combining the systems of shearlets associated with the 3 pyramidal regions \mathcal{P}_d , $d = 1, 2, 3$, together with a coarse scale system. To ensure the regularity and decay of the system, the elements of the shearlet systems overlapping the boundaries of the pyramidal regions \mathcal{P}_d in the Fourier domain need to be slightly modified. Precisely, we define the *3D shearlet systems for* $L^2(\mathbb{R}^3)$ as the collections

$$\begin{aligned} & \{\phi_k : k \in \mathbb{Z}^3\} \cup \left\{ \tilde{\psi}_{j,\ell,k,d} : j \geq 0, |\ell_1| < 2^j, |\ell_2| \leq 2^j, k \in \mathbb{Z}^3, d = 1, 2, 3 \right\} \\ & \cup \left\{ \tilde{\psi}_{j,\ell,k} : j \geq 0, \ell_1, \ell_2 = \pm 2^j, k \in \mathbb{Z}^3 \right\} \end{aligned} \quad (8)$$

consisting of:

- the *coarse-scale shearlets* $\{\phi_k = \phi(\cdot - k) : k \in \mathbb{Z}^3\}$, where ϕ is given by (1);
- the *interior shearlets* $\{\tilde{\psi}_{j,\ell,k,d} = \psi_{j,\ell,k}^{(d)} : j \geq 0, |\ell_1||\ell_2| < 2^j, k \in \mathbb{Z}^3, d = 1, 2, 3\}$, where $\psi_{j,\ell,k}^{(d)}$ is given by (6);
- the *boundary shearlets* $\{\tilde{\psi}_{j,\ell,k,d} : j \geq 0, |\ell_1| < 2^j, \ell_2 = \pm 2^j, k \in \mathbb{Z}^3, d = 1, 2, 3\}$ and $\{\tilde{\psi}_{j,\ell,k} : j \geq 0, \ell_1, \ell_2 = \pm 2^j, k \in \mathbb{Z}^3\}$, obtained by joining together slightly modified versions of $\psi_{j,\ell,k}^{(1)}$, $\psi_{j,\ell,k}^{(2)}$ and $\psi_{j,\ell,k}^{(3)}$, for $\ell_1, \ell_2 = \pm 2^j$. We refer to Ref.7 for details. Here it suffices to observe that the boundary shearlets are both compactly supported and smooth in the frequency domain.

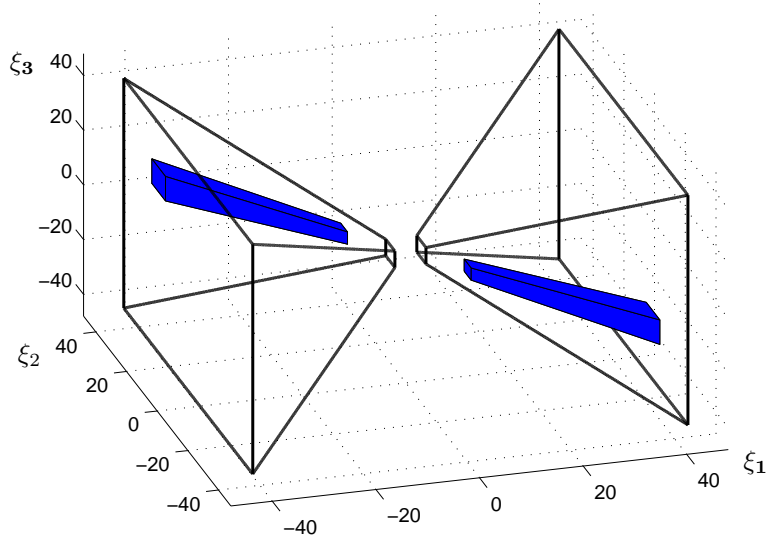


Figure 1. Frequency support of a representative shearlet function $\psi_{j,\ell,k}^{(1)}$, inside the pyramidal region \mathcal{P}_1 . The orientation of the support region is controlled by $\ell = (\ell_1, \ell_2)$; its shape is becoming more elongated as j increases ($j = 4$ in this plot)

For brevity, in the following we will denote the system of shearlets (8) using the notation:

$$\{s_\mu, \mu \in M\}, \quad (9)$$

where $M = \mathbb{Z}^3 \cup M_I \cup M_B$, $s_\mu = \phi_\mu$ if $\mu \in \mathbb{Z}^3$ and $s_\mu = \tilde{\psi}_\mu$ if $\mu \in M_I \cup M_B$, and M_I, M_B are the indices associated with the interior shearlets and the boundary shearlets, respectively, given by

- $M_I = \{\mu = (j, \ell_1, \ell_2, k, d) : j \geq 0, |\ell_1| \& |\ell_2| < 2^j, k \in \mathbb{Z}^3, d = 1, 2, 3\}$
- $M_B = \{\mu = (j, \ell_1, \ell_2, k, d) : j \geq 0, |\ell_1| < 2^j, \ell_2 = \pm 2^j, k \in \mathbb{Z}^3, d = 1, 2, 3\} \cup \{\mu = (j, \ell_1, \ell_2, k) : j \geq 0, \ell_1, \ell_2 = \pm 2^j, k \in \mathbb{Z}^3\}$

We have the following result.⁷

THEOREM 2.1. *The 3D shearlet system (9) is a Parseval frame for $L^2(\mathbb{R}^3)$. In addition, the elements of this systems are C^∞ and band-limited.*

3. 3D X-RAY DATA RECOVERY VIA SHEARLET DECOMPOSITION

One of the main results from Ref. 6 is a decomposition formula allowing one to recover a function $f \in L^2(\mathbb{R}^3)$ from the values of its X-ray transform using the shearlet representation. In order to present this result, we need to introduce some definitions.

For a rational number $\alpha < 3$, the *Riesz potential* I^α in \mathbb{R}^3 is the operator and $I^\alpha : C^\infty(\mathbb{R}^3) \rightarrow C^\infty(\mathbb{R}^3)$, defined by $\widehat{I^\alpha f}(\xi) = |\xi|^{-\alpha} \hat{f}(\xi)$. Hence we define a new collection of functions $\{U_\mu : \mu \in M\}$ associated with shearlet system (9), whose elements are defined by

$$U_\mu = 2^{-j} P I^{-1} s_\mu. \quad (10)$$

Note that, while the functions s_μ take values on \mathbb{R}^3 , the new functions U_μ are defined in the tangent bundle \mathcal{T} associated with the X-ray transform. The factor 2^{-j} in the definition of U_μ is useful to control the norm size,

which otherwise would increase with the scale parameters j due to the action of the Riesz potential operator on f . Indeed, one can show⁶ that the functions $\{U_\mu : \mu \in M\}$ form a frame for $L^2(\mathcal{T})$.

We can now state the following result.⁷

THEOREM 3.1. *Let $\{s_\mu : \mu \in M\}$ be the Parseval frame of shearlets (9) and $\{U_\mu : \mu \in M\}$ the system defined by (10). For all $f \in L^2(\mathbb{R}^3)$ the following representation holds:*

$$f = 2^{-1} \sum_{\mu} 2^j [Pf, U_\mu] s_\mu,$$

where $[\cdot, \cdot]$ is the inner product in $L^2(\mathcal{T})$.

Thanks to the ability of the shearlet representation to approximate piecewise smooth functions with optimal efficiency, this decomposition formula offers a very effective framework to reconstruct functions in this class from their X-ray projections. To state the precise result, let us suppose that the observed 3D X-ray transform of a function f is corrupted by white Gaussian noise as:

$$Y = Pf + \varepsilon W, \tag{11}$$

where W is a Wiener sheet and ε is measuring the noise level. This means that each measurement $[Y, U_\mu]$ of the observed data is normally distributed with mean $[Pf, U_\mu]$ and variance $\varepsilon^2 \|U_\mu\|_{L^2(\mathcal{T})}^2$.

Projecting the data (11) onto the system $\{U_\mu : \mu \in M\}$ and rescaling, from Theorem 3.1 we obtain that

$$\begin{aligned} 2^j [Y, U_\mu] &= 2^j [Pf, U_\mu] + \varepsilon 2^j [W, U_\mu] \\ &= 2 \langle f, s_\mu \rangle + \varepsilon 2^j n_\mu, \end{aligned} \tag{12}$$

where n_μ is a (non-i.i.d.) Gaussian noise with zero mean and variance $\sigma_\mu = \|U_\mu\|_2$. This shows that, to estimate f , we need to estimate the shearlet coefficients $\{\langle f, s_\mu \rangle\}$, $\mu \in M$, from the data $\{[Y, U_\mu]\}$. This estimate can be accomplished by an appropriate thresholding rule. Namely, let $\mathcal{N}(\varepsilon) = M_1(\varepsilon) \cup N_0(\varepsilon)$ be the *significant shearlet coefficients* (note the dependence on the noise level ε) where

$$N_0(\varepsilon) = \{\mu = k \in \mathbb{Z}^3 : |k| \leq 2^{2j+1}\}, \text{ and}$$

$$M_1(\varepsilon) = \{\mu = (j, \ell, k, d) : j_0 < j \leq j_1, |k| \leq 2^{2j+1}, d = 1, 2, 3\},$$

with $j_0 = \frac{2}{15} \log_2(\varepsilon^{-1})$ and $j_1 = \frac{1}{3} \log_2(\varepsilon^{-1})$. Hence we define the estimator \tilde{f} of the function f by

$$\tilde{f} = \sum_{\mu \in \mathcal{N}(\varepsilon)} \tilde{c}_\mu s_\mu, \tag{13}$$

where the coefficients \tilde{c}_μ are obtained by the rule

$$\tilde{c}_\mu = T_s(2^j [Y, U_\mu], \varepsilon \sqrt{2 \log(\#\mathcal{N}(\varepsilon))} 2^j \sigma_\mu), \tag{14}$$

and $T_s(y, t) = \text{sgn}(y)(|y| - t)_+$ is the soft thresholding function.

We can now state the main result about the recovery of f from noisy X-ray data. For a fixed constant $A > 0$, we denote by $\mathcal{M}(A)$ the class of indicator functions of sets $B \subset [0, 1]^3$ whose boundary Σ is twice differentiable and can be written as $\bigcup_{\alpha} \Sigma_{\alpha}$, where α ranges over a finite index set and $\Sigma_{\alpha} = \{(v, E_{\alpha}(v)), v \in V_{\alpha} \subset \mathbb{R}^2\}$, such that $\|E_{\alpha}\|_{C^2(V_{\alpha})} \leq A$ for all α . Also, let $C_c^2([0, 1]^3)$ be the collection of twice differentiable functions supported inside $[0, 1]^3$. Hence, we define the set $\mathcal{E}^2(A)$ of *functions which are C^2 away from a C^2 surface* as the collection of functions of the form

$$f = f_0 + f_1 \chi_B,$$

where $f_0, f_1 \in C_c^2([0, 1]^3)$, $B \in \mathcal{M}(A)$ and $\|f\|_{C^2} = \sum_{|\alpha| \leq 2} \|D^{\alpha} f\|_{\infty} \leq 1$. We have the following result from Ref. 6.

THEOREM 3.2. *Let $f \in \mathcal{E}^2(A)$ be the solution of the problem $Y = Rf + \varepsilon W$ and \tilde{f} be the approximation to f given by the formulas (13) and (14). Then there is a constant $C > 0$ such that*

$$\sup_{\mathcal{E}^2(A)} E\|\tilde{f} - f\|_2^2 \leq C \log(\varepsilon^{-1}) \varepsilon^{\frac{2}{3}}, \quad \text{as } \varepsilon \rightarrow 0,$$

where E is the expectation operator.

Furthermore, no estimator can achieve a rate better than $\varepsilon^{\frac{2}{3}}$ uniformly over $\mathcal{E}^2(A)$, so that this estimator is essential optimal for functions in this class.

4. RESULTS

A 3D Shepp-Logan Phantom and a “star” data set composed of various ellipsoids was created that allowed us to create synthetic X-ray data. We simulated the X-ray data acquisition in a helical sampling scheme that corresponds to one of classical acquisition geometries schemes used in actual CT devices.¹⁰ In particular, we used the implementation of the Katsevich inversion formula proposed by Wunderlich.¹⁶ Figure 2 illustrates an example of such X-ray data collected for the Phantom and its 3D reconstruction.

In our experiments, we added white Gaussian noise with standard deviation of $\sigma = 0.02$ to the X-ray data of the Phantom and $\sigma = 0.03$ to the X-ray data of the “star”. For the $N \times N \times N$ image datacubes, we assessed the performance of our algorithm by using the *peak signal-to-noise ratio* (PSNR), measured in decibels (dB), given as

$$PSNR = 20 \log_{10} \frac{255N}{\|f - \tilde{f}\|_F},$$

where $\|\cdot\|_F$ is the Frobenius norm, f is the known image datacube, and \tilde{f} is the noisy or estimated image datacube. Using this measure, the noisy x-rays datasets resulted in non-regularized reconstructions that had a PSNR of 26.47 dB and 28.94 dB, respectively, for the Phantom and “star” datasets.

The shearlet¹⁴ regularization technique was implemented by estimating the standard deviation of the noise for each decomposition level using a Monte Carlo simulation and the thresholding parameters were chosen to be four times the estimated standard deviation of the noise for the finest decomposition scales and three times the estimated standard deviations of the remain decomposition levels.

The results of the shearlet-based reconstructions are shown in Figures 3 to 5. The shearlet-based estimated 3D data cubes have a PSNR of 36.46 dB for the Phantom and of 38.04 dB for the “star”. For comparison purposes, we implemented a wavelet-based regularized reconstruction in a similar manner. The results of the wavelet-based estimated 3D data cubes have a PSNR of 31.28 dB for the Phantom and of 35.48 dB for the “star”. Besides not performing as well in terms of the measure of PSNR, the wavelet-based results clearly display more severe artifacts that are blocky in nature.

5. CONCLUSION

In this work, we have shown that the shearlet representation provides a useful formula for the reconstruction of 3D objects from their noisy X-ray projections. This shearlet-based regularization yields a theoretical near-optimal rate of convergence in estimating piecewise smooth objects from 3D X-ray projections which are corrupted by white Gaussian noise. We have demonstrated that this concept is viable for realistic data collection schemes and have shown the method to perform better than methods which rely on non-directionally oriented representations such as the wavelet representation.

Acknowledgments

D.L. acknowledges support from NSF grants DMS 1005799 and DMS 1008900; K.G. acknowledges support from NSF grant DMS 1008900.

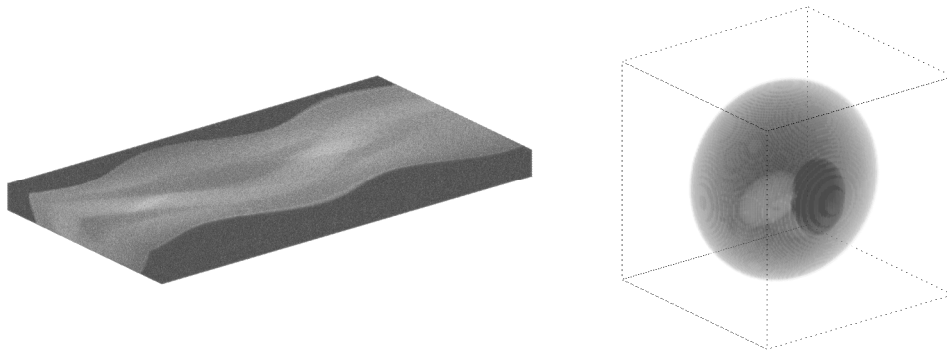


Figure 2. The image on the left is a display of the helical collected x-ray data. The image on the right is a reconstructed 3D Phantom from such data.

REFERENCES

1. E. J. Candès, and D. L. Donoho, Recovering edges in ill-posed inverse problems: optimality of curvelet frames, *Annals Stat.* **30**(3) (2002), 784–842.
2. F. Colonna, G.R. Easley, K. Guo, D. Labate, Radon transform inversion using the shearlet representation, *Appl. Comput. Harmon. Anal.* **29**(2) (2010), 232–250.
3. D. L. Donoho, Nonlinear solution of linear inverse problem by wavelet- vaguelette decomposition, *Appl. Comput. Harmon. Anal.* **2** (1995), 101–126.
4. G. R. Easley, F. Colonna, D. Labate, Improved Radon Based Imaging using the Shearlet Transform, *Proc. SPIE, Independent Component Analyses, Wavelets, Unsupervised Smart Sensors, and Neural Networks II*, **7343** (2009), Orlando.
5. G. R. Easley, D. Labate, and W-Q Lim, Sparse Directional Image Representations using the Discrete Shearlet Transform, *Appl. Comput. Harmon. Anal.* **25**(1), 25–46 (2008).
6. K. Guo, and D. Labate, Optimal recovery of 3D X-ray tomographic data using the shearlet representation, *Advances in Computational Mathematics* **39**(2), 227–255 (2013).
7. K. Guo, and D. Labate, The Construction of Smooth Parseval Frames of Shearlets, *Math. Model. Nat. Phenom.* **8**(1), 82–105 (2013).
8. K. Guo, W. Lim, D. Labate, G. Weiss, E. Wilson, Wavelets with composite dilations and their MRA properties, *Appl. Computat. Harmon. Anal.* **20**, 231–249 (2006).
9. S. Helgason, *The Radon Transform*, Birkhäuser, Boston, 1980.
10. C. Kao, E. Sidky, P. La Riviere and X. Pan, Some Recent Developments in Reconstruction Algorithms for Tomographic Imaging in: *Principles and Advanced Method in Medical Imaging and Image Analysis*, World Scientific Publishing, 2008.
11. G. Kutyniok and D. Labate, Resolution of the Wavefront Set using Continuous Shearlets, *Trans. Amer. Math. Soc.* **361**, 2719–2754 (2009).
12. D. Labate, W. Lim, G. Kutyniok and G. Weiss, Sparse Multidimensional Representation using Shearlets, Wavelets XI (San Diego, CA, 2005), 254-262, *SPIE Proc. 5914*, SPIE, Bellingham, WA, 2005.
13. F. Natterer, and F. Wübbeling, *Mathematical Methods in Image Reconstruction*, SIAM Monographs on Mathematical Modeling and Computation, Philadelphia, 2001.
14. P. S. Negi, D. Labate. 3D discrete shearlet transform and video processing, *IEEE Trans. Image Process.* **21**(6), 944–2954 (2012).

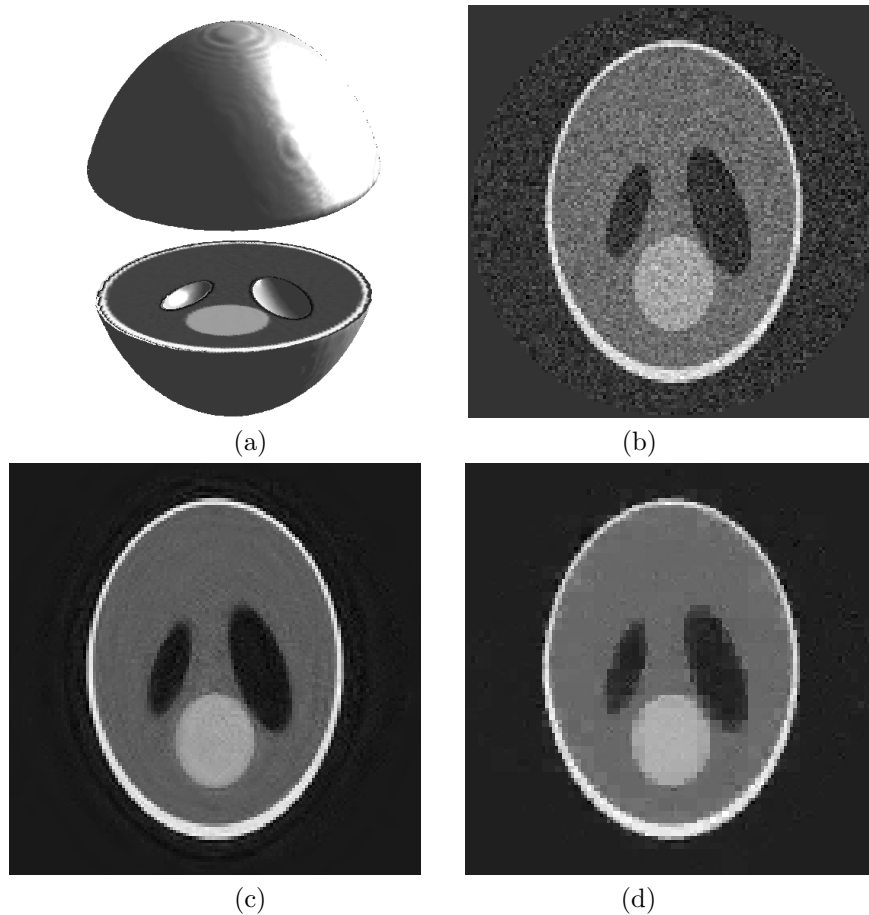


Figure 3. (a) An illustration depicting where the sectional image slice shown in (b) comes from in the 3D Phantom reconstruction. (b) A noisy 3D x-ray reconstruction image slice (PSNR = 26.47 dB). (c) An image slice of the 3D shearlet based estimate (PSNR = 36.46 dB). (d) An image slice of the 3D wavelet based estimate (PSNR = 31.28 dB).

15. J. Radon, Über die Bestimmung von Funktionen durch ihre Integralwerte längs gewisser Mannigfaltigkeiten, *Berichte Sächsische Akademie der Wissenschaften, Leipzig, Math.-Phys. Kl.* **69**, 262–267, reprinted in ⁹, 177–192, 1917.
16. A. J. Wunderlich, *The Katsevich Inversion Formula for Cone-Beam Computed Tomography*, Department of Mathematics, Oregon State University, 2006.

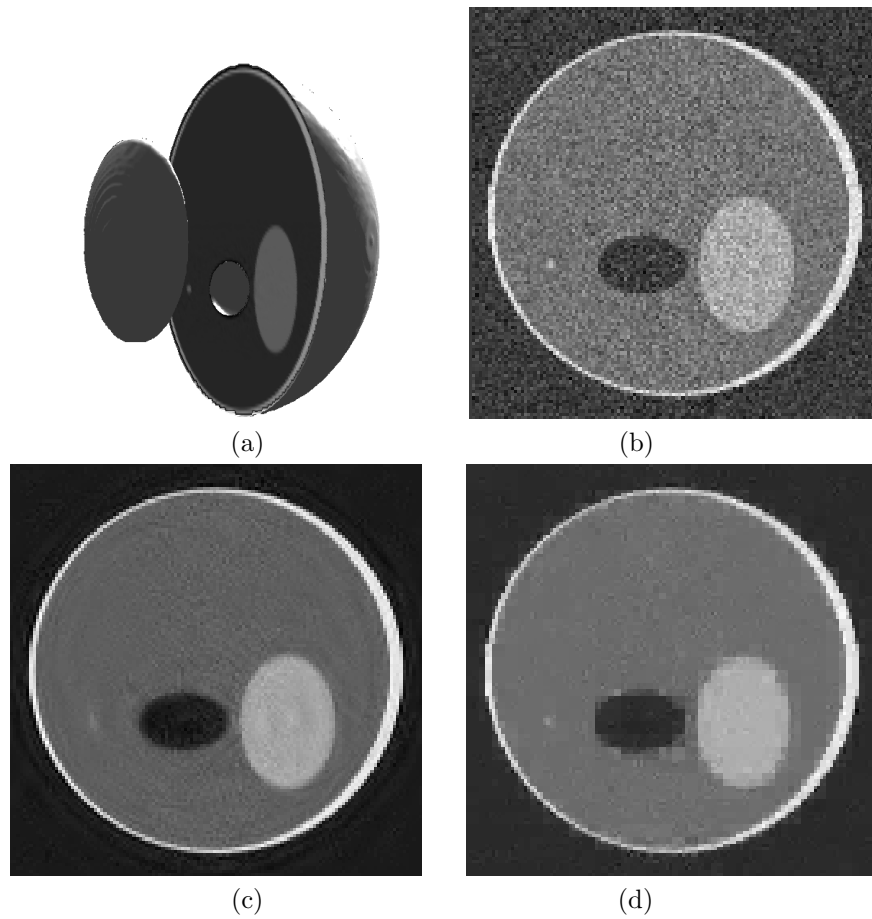


Figure 4. (a) An illustration depicting where the sectional image slice shown in (b) comes from in the 3D Phantom reconstruction. (b) A noisy 3D x-ray reconstruction image slice (PSNR = 26.47 dB). (c) An image slice of the 3D shearlet based estimate (PSNR = 36.46 dB). (d) An image slice of the 3D wavelet based estimate (PSNR = 31.28 dB).

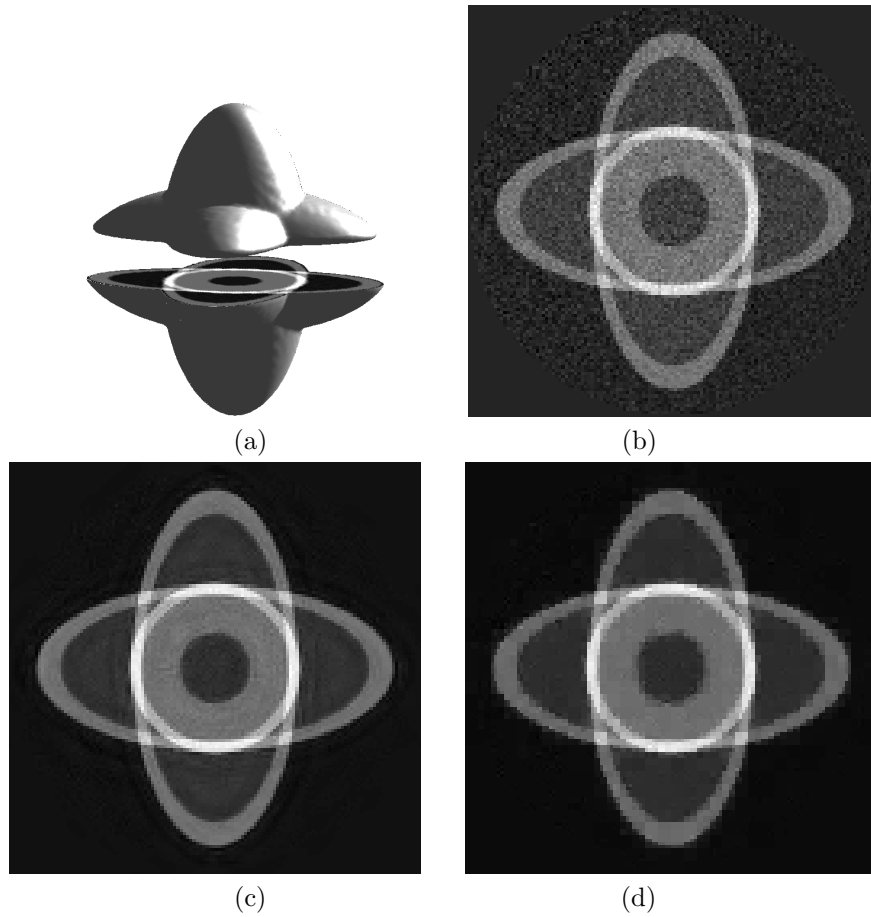


Figure 5. (a) An illustration depicting where the sectional image slice shown in (b) comes from in the 3D “star” reconstruction. (b) A noisy 3D x-ray reconstruction image slice (PSNR = 28.94 dB). (c) An image slice of the 3D shearlet based estimate (PSNR = 38.04 dB). (d) An image slice of the 3D wavelet based estimate (PSNR = 35.48 dB).